Impact of the QCD four-quark condensate on in-medium spectral changes of light vector mesons

S. Zschocke,[1] O.P. Pavlenko,[2] and B. Kämpfer[1]
[1] *Forschungszentrum Rossendorf, PF 510119, 01314 Dresden, Germany*
[2] *Institute for Theoretical Physics, 03143 Kiev - 143, Ukraine*

Abstract

Within the Borel QCD sum rule approach at finite baryon density we study the role of the four-quark condensates for the modifications of the vector mesons ρ, ω and ϕ in nuclear matter. We find that in-medium modifications of the ρ and ω mesons are essentially dominated by the dependence of the 4-quark condensate on the nucleon density. In particular, the numerical value of a parameter (κ_N), which describes the strength of the density dependence of the 4-quark condensate beyond the mean-field approximation, governs the decrease of the ρ mass as a function of the density. For the ω meson the sign of the in-medium mass shift is changed by variations of κ_N. To study consistently the in-medium broadening of the light vector mesons we employ ρN and ωN scattering amplitudes derived recently from a covariant unitary coupled channel approach adjusted to pion- and photo-induced reactions. In contrast to the ρ and ω mesons, the in-medium mass of the ϕ meson is directly related to the chiral (strange) quark condensate. Measurements of the vector meson spectral change in heavy-ion collisions with HADES can shed light on the yet unknown density dependence of the 4-quark condensate.

PACS numbers: 14.40.Cs, 21.65.+f, 11.30.Rd, 24.85.+p

I. INTRODUCTION

Changes of the vector meson properties in strongly interacting matter at finite baryon density and temperature are presently of great interest, both theoretically and experimentally. In particular, the current heavy-ion experiments with the detector HADES [1] at the heavy-ion synchrotron SIS18 (GSI, Darmstadt) are mainly aimed at measuring in-medium modifications of light vector meson via the e^+e^- decay channel with high accuracy. One of the primary goals of the future experiments planned at SIS100/200 is also to study very dense baryon matter and the expected strong changes of the in-medium hadrons.

It is widely believed that the in-medium spectral change of the light mesons is related to the chiral symmetry restoration at finite temperature and baryon density. There are indeed various theoretical indications concerning an important sensitivity of the meson spectral density on the partial restoration of the chiral symmetry in a hot/dense nuclear medium. For instance, at finite temperature the vector and axial-vector meson correlators become mixed in accordance with in-medium Weinberg sum rules [2, 3]. Such a mixing causes an increasing degeneracy of vector and axial-vector spectral functions which would manifest themselves as a decrease of the ρ and a_1 meson mass splitting. Similarly, the degeneracy of scalar (σ channel) and pseudo-scalar (π channel) correlators found in lattice QCD [4] can lead to a considerable enhancement of the σ meson spectral function at finite temperature and density [5].

In spite of substantial efforts undertaken to understand the nature of vector mesons in a dense medium there is so far no unique and widely accepted quantitative picture of their in-medium behavior. The Brown and Rho conjecture [6] on the direct interlocking of vector meson masses and chiral quark condensate $\langle \overline{q}q \rangle_n$ supplemented by the "vector manifestation" of chiral symmetry in medium [7, 8] predict a strong and quantitatively the same decrease of the in-medium ρ and ω meson masses.

At the same time, model calculations based on various effective Lagrangians (cf. [9]) predict rather moderate and different mass shifts for ρ and ω mesons in a dense medium. In order "to match" both sets of predictions one has to go beyond simplifications made in the above mentioned approaches: The in-medium vector meson modification is governed not only by $\langle \overline{q}q \rangle_n$ but also by condensates of higher order to be evaluated beyond mean-field approximation. Further, effective Lagrangians are dealing with the scattering amplitudes in free space, but effects related to the in-medium change of the QCD condensates should be included [10].

The very consistent way to incorporate in-medium QCD condensates is through QCD sum rules (QSR). The QSR for vector mesons in nuclear matter were first developed in [11], where within a simple parameterization of the spectral density in terms of a delta function at the resonance peak an agreement with the Brown-Rho scaling, i.e. the same dropping of the ρ and ω meson masses, in nuclear matter was obtained. While the zero-width approximation for the resonance spectral density is successful in vacuum [12], such an approximation is not well grounded for the in-medium mesons which can undergo rather strong inelastic scatterings off the surrounding nucleons. For realistic in-medium QSR evaluations one needs to take into account the finite meson widths including collision broadening effects. The important impact of the finite width was studied, e.g., in [13] using a plausible ansatz for the in-medium spectral density. As shown in this QSR analysis, there is no inevitable necessity for in-medium dropping of the vector meson masses, but the global changes of mesons like mass shift and width broadening turn out to be correlated in nuclear matter. To avoid too many unknown parameters in the QSR equation and to make more definite predictions one has to specify in a detailed manner the ansatz for the hadron spectral density. As we show below such a specification for ρ and ω vector mesons can be done basing on an effective Lagrangian approach which gives a realistic behavior of the ρN and ωN scattering amplitudes.

As well known, QSR in nuclear matter contain also an uncertainty related to the poorly known density dependence of the four-quark condensate. The majority of the QSR evaluations employs mean-field approximations for the in-medium 4-quark condensate, i.e. its density dependence is simply governed by the chiral condensate squared. At the same time, as pointed out in [14] the in-medium mass shift of the ρ and ω mesons is dominated by the dependence of the 4-quark condensate on density. In particular, the sign of the ω meson mass shift is changed by the variation of the strength of the density dependence of the 4-quark condensate beyond mean-field approximation. This result was confirmed in [15], where the ω meson spectral density was constrained within a general form of the in-medium ω meson propagator including collision broadening via the imaginary part of the ωN scattering amplitude delivered by an effective chiral Lagrangian [16].

A direct observation of the ω meson spectral change via the e^+e^- decay channel appears to be an experimental challenge in heavy-ion collisions at SIS18 energies. Both transport code simulations [17] and a hydrodynamical model approach [18] point to a considerable contribution of the reaction $\pi^+\pi^- \to \rho \to e^+e^-$ into dilepton spectra in the wanted region. A chance to separate e^+e^- pairs from in-medium ρ and ω mesons crucially depends on the quantitative details of their mass shift and width broadening in nuclear matter. This gives rise to a strong request from the experimental side to find out the ρ and ω meson in-medium spectral changes simultaneously on a unique basis including self-consistently effects of the QCD condensates and collision broadening in nuclear matter.

In the present paper we study systematically within the Borel QSR the important role of the 4-quark condensate for spectral modifications of the ρ and ω mesons in baryon matter. Being still within the low-density expansion we go beyond the mean-field approximation and vary the strength of the density dependence of the 4-quark condensate. Concerning the in-medium meson spectral density entering the hadronic part of the QSR evaluation we use a constraint motivated by the general structure of the vector meson propagator with finite in-medium width of ρ and ω mesons reflecting the scattering of vector mesons off nucleons the in nuclear medium. Seeking realistic ρN and ωN scattering amplitudes we employ the results of the recent covariant unitarized coupled channel approach [19] which satisfactorily describes the experimental pion- and photon-nucleon scattering data.

We find that in-medium modifications of the ρ and ω mesons are indeed dominated by the dependence of the 4-quark condensate on density. In particular, the numerical value of a parameter, which describes the strength of the linear density dependence of the 4-quark condensate, governs the decrease of the ρ meson mass as a function of density. For the ω meson the sign of the in-medium mass shift is changed by variations of this parameter. Since the difference of the vector and axial-vector correlators is proportional to the 4-quark condensate the sign of the vector meson mass shift, measured via the e^+e^- channel, can serve as a tool for determining how fast nuclear matter approaches the chiral symmetry restoration with increasing baryon density.

Our paper is organized as follows. In section II we recapitulate the necessary equations and formulate the Borel QCD sum rule. The systematic evaluation of this sum rule is presented in section III for ρ and ω mesons. As supplement, we consider in section IV the case of the ϕ meson. The summary and a discussion can be found in section V. Appendices A and B summarize the vacuum ρ self-energy and the ρ, ω meson-nucleon scattering amplitudes, respectively. In Appendix C we report on some technical details.

II. QCD SUM RULE EQUATION

For the sake of self-containment we list here the relevant equations for the Borel QCD sum rule which our evaluations are based on.

A Dispersion relation

Within QCD sum rules the in-medium vector mesons $V = \rho, \omega$ are considered as a resonances in the current-current correlation function

$$\Pi_{\mu\nu}(q,n) = i \int d^4x \; \mathrm{e}^{iq\cdot x} \langle \mathcal{T} \; J_\mu(x) \; J_\nu(0) \rangle_n \; , \tag{2.1}$$

where $q_\mu = (E, \mathbf{q})$ is the meson four momentum, $\mathcal{T}$ denotes the time ordered product of the respective meson current operators $J_\mu(x)$, and $\langle \cdots \rangle_n$ stands for the expectation value in medium. In what follows, we focus on the ground state of low-density baryon matter approximated by a Fermi gas with nucleon density n. We consider isospin symmetric nuclear matter, where the $\rho - \omega$ mixing effect is negligible [20]. In terms of quark field operators, the vector meson currents are given by $J_\mu = \frac{1}{2}(\bar{\mathrm{u}}\gamma_\mu \mathrm{u} \mp \bar{\mathrm{d}}\gamma_\mu \mathrm{d})$, where the negative (positive) sign is for the ρ (ω) meson. The correlator (2.1) can be reduced to $\frac{1}{3}\Pi^\mu_\mu(q^2, n) = \Pi^{(V)}(q^2, n)$ for a vector meson at rest, $\mathbf{q} = 0$, in the rest frame of matter. In each of the vector meson channels the corresponding correlator $\Pi^{(V)}(q^2, n)$ satisfies the twice subtracted dispersion relation, which can be written with $Q^2 \equiv -q^2 = -E^2$ as

$$\frac{\Pi^{(V)}(Q^2)}{Q^2} = \frac{\Pi^{(V)}(0, n)}{Q^2} - \Pi^{(V)\prime}(0) - Q^2 \int\limits_0^\infty ds \frac{R^{(V)}(s)}{s(s + Q^2)} \, , \tag{2.2}$$

with $\Pi^{(V)}(0, n) = \Pi^{(V)}(q^2 = 0, n)$ and $\Pi^{(V)\prime}(0) = \frac{\mathrm{d}\Pi^{(V)}(q^2)}{\mathrm{d}q^2}|_{q^2=0}$ as subtraction constants, and $R^{(V)}(s) \equiv -\frac{1}{\pi}\frac{\mathrm{Im}\Pi^{(V)}(s,n)}{s}$.

As usual in QCD sum rules [11, 12], for large values of Q^2 one can evaluate the r.h.s. of eq. (2.1) by the operator product expansion (OPE) leading to

$$\frac{\Pi^{(V)}(Q^2)}{Q^2} = -c_0 \ln(Q^2) + \sum_{i=1}^{\infty} \frac{c_i}{Q^{2i}} \, , \tag{2.3}$$

where the coefficients c_i include the Wilson coefficients and the expectation values of the corresponding products of the quark and gluon field operators, i.e. condensates.

Performing a Borel transformation of the dispersion relation (2.2) with appropriate parameter M^2 and taking into account the OPE (2.3) one gets the basic QSR equation

$$\Pi^{(V)}(0, n) + \int\limits_0^\infty ds \, R^{(V)}(s) \, \mathrm{e}^{-s/M^2} = c_0 M^2 + \sum_{i=1}^{\infty} \frac{c_i}{(i-1)! M^{2(i-1)}} \, . \tag{2.4}$$

The advantage of the Borel transformation is (i) the exponential suppression of the high-energy part of $R^V(s)$, and (ii) the possibility to suppress higher-order contributions to the r.h.s. sum. Choosing sufficiently large values of the internal technical parameter M one can truncate the sum in controlled way, in practice at $i = 3$. The general structure of the coefficients c_i up to $i = 3$ is given, for instance, in [11, 21, 22].

B QCD condensates

In order to calculate the density dependence of the condensates entering the coefficients c_i we employ the standard linear density approximation, which is valid for not too large density. This gives for the chiral quark condensate $\langle \overline{q}q \rangle_n = \langle \overline{q}q \rangle_0 + \frac{\sigma_N}{2m_q} n$, where we assume here isospin symmetry for the light quarks, i.e. $m_q = m_u = m_d = 5.5$ MeV and $\langle \bar{q}q \rangle_0 = \langle \bar{u}u \rangle_0 = \langle \bar{d}d \rangle_0 = -(0.24\,\mathrm{GeV})^3$. The nucleon sigma term is $\sigma_N = 45$ MeV. The gluon condensate is obtained as usual employing the QCD trace anomaly $\langle \frac{\alpha_s}{\pi} \mathrm{G}^2 \rangle_n = \langle \frac{\alpha_s}{\pi} \mathrm{G}^2 \rangle_0 - \frac{8}{9} M_N^0\, n$, where $\alpha_s = 0.38$ is the QCD coupling constant and $M_N^0 = 770$ MeV is the nucleon mass in the chiral limit. The vacuum gluon condensate is $\langle \frac{\alpha_s}{\pi} G^2 \rangle_0 = (0.33\,\mathrm{GeV})^4$.

The coefficient c_3 in eq. (2.4) contains also the mass dimension-6 4-quark condensates (cf. [23] for a recent calculation of corresponding matrix elements) $\langle (\bar{q}\gamma_\mu \lambda^a q)^2 \rangle_n$, $\langle (\bar{u}\gamma_\mu \lambda^a u)(\bar{d}\gamma^\mu \lambda^a d) \rangle_n$, $\langle (\bar{q}\gamma_\mu \lambda^a q)(\bar{s}\gamma^\mu \lambda^a s) \rangle_n$, and $\langle (\overline{q}\gamma_\mu \gamma^5 \lambda^a q)^2 \rangle_n$ which are common for ρ and ω mesons. On this level, ρ and ω mesons differ only by the condensate $\pm 2 \langle (\bar{u}\gamma_\mu \gamma_5 \lambda^a u)(\bar{d}\gamma^\mu \gamma_5 \lambda^a d) \rangle_n$ (cf. [22]), causing the small $\rho - \omega$ mass splitting in vacuum [24]. The standard approach to estimate the density dependence of the 4-quark condensates consists in the use of the mean-field approximation. Within such an approximation the 4-quark condensates are proportional to $\langle \overline{q}q \rangle_n^2$ and their density dependence is actually governed by the square of the chiral quark condensate. Keeping in mind the important role of the 4-quark condensate for the in-medium modifications of the vector mesons, we go beyond this approximation and employ the following parameterization [14]

$$\langle (\bar{q}\gamma_\mu \gamma^5 \lambda^a q)^2 \rangle_n = \frac{16}{9} \langle \overline{q}q \rangle_0^2\, \hat{\kappa}_0 \, \left[1 + \frac{\hat{\kappa}_N}{\hat{\kappa}_0} \frac{\sigma_N}{m_q \langle \bar{q}q \rangle_0}\, n \right] . \tag{2.5}$$

In vacuum, $n = 0$, the parameter $\hat{\kappa}_0$ reflects a deviation from the vacuum saturation assumption. The case $\hat{\kappa}_0 = 1$ corresponds obviously to the exact vacuum saturation [25] as used, for instance, in [21]. To control the deviation of the in-medium 4-quark condensate from the mean-field approximation we introduce the parameter $\hat{\kappa}_N$. The limit $\hat{\kappa}_N = \hat{\kappa}_0$ recovers the mean-field approximation, while the case $\hat{\kappa}_N > \hat{\kappa}_0$

($\hat{\kappa}_N < \hat{\kappa}_0$) is related to the stronger (weaker) density dependence compared to the mean-field approximation.

An analog procedure applies for the other 4-quark condensates, each with its own $\hat{\kappa}_0$ and $\hat{\kappa}_N$, which sum up to a parameter κ_0 and a parameter κ_N. Below we vary the poorly constrained parameter κ_N to estimate the contribution of the 4-quark condensates to the QSR with respect to the main trends of the in-medium modification of the vector meson spectral function. As seen in eq. (2.5) and eq. (2.9) below, κ_N parameterizes the density dependence of the summed 4-quark condensates; κ_0 is adjusted to the vacuum masses. Strictly speaking, κ_0 and κ_N differ for ρ and ω mesons due to contributions of the above mentioned flavor-mixing condensate; in addition, in medium a twist-4 condensate make further ρ and ω to differ [22]. However, the differences can be estimated to be sub-dominant. Therefore, we use in the present work one parameter κ_N, keeping in mind that it may slightly differ for different light vector mesons.

Using the above condensates and usual Wilson coefficients one gets as relevant terms for mass dimension ≤ 6 and twist ≤ 2

$$c_0 = \frac{1}{8\pi^2}\left(1 + \frac{\alpha_s}{\pi}\right) , \tag{2.6}$$

$$c_1 = -\frac{3m_q^2}{4\pi^2} , \tag{2.7}$$

$$c_2 = m_q\langle\overline{q}q\rangle_0 + \frac{\sigma_N}{2}\, n + \frac{1}{24}\left[\langle\frac{\alpha_s}{\pi}G^2\rangle_0 - \frac{8}{9}M_N^0\, n\right] + \frac{1}{4}A_2 M_N\, n , \tag{2.8}$$

$$c_3 = -\frac{112}{81}\pi\, \alpha_s\, \kappa_0\, \langle\overline{q}q\rangle_0^2 \left[1 + \frac{\kappa_N}{\kappa_0}\frac{\sigma_N}{m_q\langle\overline{q}q\rangle_0}\, n\right] - \frac{5}{12}A_4 M_N^3\, n. \tag{2.9}$$

The last terms in $c_{2,3}$ correspond to the derivative condensates from non-scalar operators as a consequence of the breaking of Lorentz invariance in the medium. These condensates are proportional to the moments $A_i = 2\int_0^1 dx\ x^{i-1}\,[q_N(x,\mu^2 + \overline{q}_N(x,\mu^2))]$ of quark and anti-quark distributions inside the nucleon at scale $\mu^2 = 1\mathrm{GeV}^2$ (see for details [11]). Our choice of the moments A_2 and A_4 is 1.02 and 0.12, respectively.

The value of κ_0 in eq. (2.5) is related to such a choice of the chiral condensate

$\langle\overline{q}q\rangle_0$ to adjust the vacuum vector meson masses. In our QSR we have used $\kappa_0 = 3$, obtaining $m_{\rho,\omega}(n=0) = 777$ MeV close to the nominal vacuum values. The ratio κ_N/κ_0 in the parameterization (2.5) is restricted by the condition $\langle(\overline{q}\gamma_\mu\lambda^a q)^2\rangle_n \leq 0$, so that one gets $0 \leq \kappa_N \leq 4$ as reasonable numerical limits when considering $n \leq n_0$, as dictated by our low-density approximation.

The case of finite baryon density and temperature has been considered in [14]. Here we focus on density effects with the reasoning that temperature effects below 100 MeV are negligible.

C Vector meson spectral density

To model the hadronic side of the QSR (2.4) we make the standard separation of the vector meson spectral density $R^{(V)}$ into resonance part and continuum contribution by means of the threshold parameter s_V

$$R^{(V)}(s,n) = F_V \, \frac{S^{(V)}(s,n)}{s} \, \Theta(s_V - s) + c_0 \, \Theta(s - s_V) \, , \tag{2.10}$$

where $S^{(V)}(s,n)$ stands for the resonance peak in the spectral function; the normalization F_V is unimportant for the following consideration. In the majority of the previous QCD sum rule evaluations, the zero-width approximation [11] or some parameterization of $S^{(V)}$ [13] are employed. In contrast to this, we use here a more realistic ansatz for the resonance spectral density $S^{(V)}$ based on the general structure of the in-medium vector meson propagator

$$S^{(V)}(s,n) = -\frac{\mathrm{Im}\,\Sigma_V(s,n)}{(s - \overset{\circ}{m}{}_V^2(n) - \mathrm{Re}\,\Sigma_V(s,n))^2 + (\mathrm{Im}\,\Sigma_V(s,n))^2} \, , \tag{2.11}$$

with $\mathrm{Re}\,\Sigma_V(s,n)$ and $\mathrm{Im}\,\Sigma_V(s,n)$ as real and imaginary part of the in-medium vector meson self-energy. An important point of our approach is that the meson mass parameter $\overset{\circ}{m}_V(n)$ becomes density dependent in nuclear matter. This dependence is determined by the QCD sum rule eq. (2.4) and mainly governed by the QCD condensates. As a result (see below) the in-medium change of the QCD condensates causes global modifications of the vector meson spectral function, in addition to the collision broadening. (An analogous approach was used in [26].) The in-medium vector meson mass is determined by the pole position of the meson propagator

$$m_V^2(n) = \overset{\circ}{m}{}_V^2(n) + \mathrm{Re}\,\Sigma_V(s = m_V^2(n), n) \,, \tag{2.12}$$

which looks similar to the vacuum case, where $n = 0$. The difference $\Delta m_V(n) \equiv m_V(n) - m_V(0)$ can be associated with the in-medium vector meson mass shift that is widely used to characterize the spectral change of mesons in matter.

Within the linear density approximation the vector meson self energy is given by

$$\Sigma_V(E, n) = \Sigma_V^{\mathrm{vac}}(E) - n\, T_{VN}(E) \,, \tag{2.13}$$

where $E = \sqrt{s}$ is the meson energy, $\Sigma_V^{\mathrm{vac}}(E) = \Sigma_V(E, n = 0)$, and $T_{VN}(E)$ is the (off-shell) forward meson-nucleon scattering amplitude in free space. The renormalized quantity $\Sigma_\rho^{\mathrm{vac}}$ is summarized in the Appendix A; for the ω meson we absorb as usual $\mathrm{Re}\Sigma_\omega^{\mathrm{vac}}$ in $\overset{\circ}{m}{}_\omega^2$ (cf. [27] for details) and put $\mathrm{Im}\Sigma_\omega^{\mathrm{vac}} = -m_\omega \Gamma_\omega \Theta(E - 3m_\pi)$ with the vacuum values of mass m_ω and width Γ_ω.

The described framework is well defined, supposed T_{VN} is reliably known. Unfortunately, the determination of T_{VN} is hampered by uncertainties (cf. results in [16] and [19]). $\mathrm{Im}T_{VN}$ is more directly accessible, while $\mathrm{Re}T_{VN}$ follows by a dispersion relation with sometimes poorly known subtraction coefficients. Since our emphasis here is to include the collision broadening and finite width effects in the spectral function, we absorb in the following $\mathrm{Re}T_{VN}$ in $\overset{\circ}{m}{}_V^2(n)$ thus neglecting a possible strong energy dependence. In such a way, the uncertainties of $\mathrm{Re}T_{VN}$ become milder since $m_V(n)$ is then mainly determined by the QSR.

We take the needed $\mathrm{Im}T_{VN}(E)$ for ρ and ω mesons from results of the detailed analysis of pion- and photon-nucleon scattering data performed recently in [19] on the footing of the Bethe-Salpeter equation approach with four-point meson-baryon contact interactions and a unitary condition for the coupled channels. Because of the presence of dynamically generated nucleon resonances, like the s-waves N(1535), N(1650) and d-wave N(1520) resonances, the vector meson-nucleon scattering amplitudes obtained in [19] exhibit rapid variations with energy (see Appendix B, Figs. 10

and 11). For the ρN channel, the dominant contribution in Im$T_{\rho\mathrm{N}}(E)$ comes from the resonances N(1535) and N(1520). Due to the rather moderate coupling of the ρN channel to N(1520), the value of the inelastic ρN scattering amplitude is comparatively small and, therefore, the ρ meson width is not significantly increased. At the same time, N(1520) is coupled strongly to the ωN channel. This causes the pronounced peak in the subthreshold region of Im$T_{\omega\mathrm{N}}(E)$. Such a peak like energy dependence differs even qualitatively from results of the chiral Lagrangian approach [16]. We do not advocate here a particular effective Lagrangian approach for the vector meson-nucleon scattering amplitudes in vacuum. Our aim is rather to demonstrate the impact of the QCD side, in particular of the in-medium 4-quark condensate, on the global vector meson spectral change in nuclear matter.

For the subtraction constants $\Pi^{(V)}(0,n)$ in eq. (2.2) we use $\Pi^{(\rho)}(0,n) = n/(4M_N)$, $\Pi^{(\omega)}(0,n) = 9n/(4M_N)$, which are actually the Thomson limit of the VN scattering processes, but also coincide with Landau damping terms elaborated in [20] for the hadronic spectral function entering the dispersion relation without subtractions. For details about the connection of subtraction constants and Landau damping term we refer the interested reader to [28].

D QCD sum rule

Taking the ratio of the eq. (2.4) to its derivative with respect to M^2, and using (2.10) one gets

$$\frac{\int\limits_0^{s_V} ds\, S^{(V)}(s,n)\, \mathrm{e}^{-s/M^2}}{\int\limits_0^{s_V} ds\, S^{(V)}(s,n)\, s^{-1}\, \mathrm{e}^{-s/M^2}} = \frac{c_0\, M^2\, [1 - \left(1 + \frac{s_V}{M^2}\right) \mathrm{e}^{-s_V/M^2}] - \frac{c_2}{M^2} - \frac{c_3}{M^4}}{c_0 \left(1 - \mathrm{e}^{-s_V/M^2}\right) + \frac{c_1}{M^2} + \frac{c_2}{M^4} + \frac{c_3}{2M^6} - \frac{\Pi^{(V)}(0,n)}{M^2}} \tag{2.14}$$

with the coefficients $c_1, \cdots, c_3$ from eqs. (2.6 $\cdots$ 2.9) and the resonance spectral function $S^{(V)}(s,n)$ from (2.11). Eq. (2.14) determines the mass parameter

$\overset{\circ}{m}_V\ (n; M^2, s_V)$ being here the subject of the QCD sum rule.

III. RESULTS OF QSR EVALUATION FOR ρ, ω MESONS

Before coming to the results we have to specify the numerical evaluation of the QCD sum rule (2.14).

A Evaluation of the sum rule

At a given baryon density n the continuum threshold s_V is determined by requiring maximum flatness of $\overset{\circ}{m}_V\ (n; M^2, s_V)$ as a function of M^2 within the Borel window $M^2_{\rm min} \cdots M^2_{\rm max}$. The minimum Borel parameter $M^2_{\rm min}$ is determined such that the terms of order $\mathcal{O}(M^{-6})$ on the OPE side eq. (2.4) contribute not more that 10% [13, 29]. Selecting such sufficiently large values of $M^2_{\rm min}$ suppresses higher-order contributions in the OPE eq. (2.4) and justifies the truncation. Typically, $M^2_{\rm min}(10\%)$ is in the order of 0.6 GeV^2. The values for $M^2_{\rm max}$ are roughly determined by the "50% rule" [22, 29], i.e., the continuum part of the hadronic side must not contribute more than 50% to the total hadronic side. According to our experience [14], $\overset{\circ}{m}_V$ is not very sensitive to variations of $M^2_{\rm max}$. We can, therefore, fix the maximum Borel parameter by $M^2_{\rm max} = 1.5\,(2.4)\,{\rm GeV}^2$ for the ω (ρ) meson, in good agreement with the "50% rule". The sensitivity of the results on these choices of the Borel window is discussed in Appendix C. Two examples of $\overset{\circ}{m}_V$ as a function of the Borel parameter M^2 are displayed in Figs. 1 and 2 for our default parameters and for $n = n_0 = 0.15$ fm^{-3}. One observes, indeed, flat curves $\overset{\circ}{m}_V\ (n; M^2, s_V)$ within the Borel window. This is a prerequisite for the stability of the following analyses.

To get finally the vector meson mass parameter $\overset{\circ}{m}_V\ (n)$ we average the quantity $\overset{\circ}{m}_V\ (n; M^2, s_V)$ within the above Borel window to get $\overset{\circ}{m}_V\ (n) = (M^2_{\rm max} - M^2_{\rm min})^{-1} \int_{M^2_{\rm min}}^{M^2_{\rm max}} dM^2\ \overset{\circ}{m}_V\ (n; M^2, s_V)$ which is used in eqs. (2.11, 2.12).

B In-medium modifications of ρ, ω masses

The results of our QSR evaluations for the density dependence of the vector meson masses $m_\rho(n)$ and $m_\omega(n)$, defined in eq. (2.12), for $\kappa_N = 1 \cdots 4$ are exhibited in Figs. 3 and 4, respectively. As seen in Fig. 3 the ρ meson mass drops with increasing nucleon density. The value of the ρ meson mass shift at given density is directly governed by the parameter κ_N, i.e. the strength of the density dependence of the 4-quark condensate. Some qualitative arguments to understand such an important role of the 4-quark condensate for the in-medium ρ meson mass shift are given in [14].

The impact of the 4-quark condensate is more pronounced for the isoscalar channel. In Fig. 4 one can observe that such a global characteristic as the sign of the ω meson mass shift is changed by a variation of the parameter κ_N. Similar to the ρ meson the density dependence of the ω meson mass $m_\omega(n)$ is mainly governed by the QCD mass-parameter $\overset{\circ}{m}_\omega (n)$ in accordance with the in-medium change of the 4-quark condensate. (This confirms previous results obtained within the zero-width approximation, which is equivalent to an evaluation of a normalized moment of the spectral function [14], and the finite width treatment in [15] based on an effective chiral Lagrangian [16].) In particular, for a weak dependence of the 4-quark condensate on density ($\kappa_N \lesssim 2$) the ω meson mass $m_\omega(n)$ is increased, while for a greater value of κ_N the ω meson mass decreases with density.

The sign of the ω meson mass shift is important with respect to the expectation to produce nuclear bound states of ω meson using suitable projectiles impinging on a nuclear target [16]. From our study one can conclude that a negative ω meson mass shift, corresponding an effective attractive potential, is caused by a strong dependence of the 4-quark condensate on density, i.e. for $\kappa_N \gtrsim 3$.

The different behavior of $m_\rho(n)$ and $m_\omega(n)$ can be traced back, to some extent, to different values of the subtraction constants $\Pi^{(\rho,\omega)}(0, n)$, as emphasized in [20]. The strikingly different vacuum widths, $\mathrm{Im}\Sigma^{\mathrm{vac}}_{\rho,\omega}$, cause further differences, in medium additionally amplified by different shapes of $T_{\rho,\omega N}$.

Our calculations also show that the main pattern of the behavior of $m_V(n)$ plotted in Figs. 3 and 4 remains stable even for the extreme cases when including $\mathrm{Re}T_{\omega N}$ or discarding $T_{\omega N}$ at all. This still points to the crucial role of the 4-quark condensate for the ρ, ω meson in-medium mass shifts. The robustness of the pattern of $m_V(n)$ as a function of the density under variations of T_{VN} can be interpreted as stringent impact of the density dependence of the condensates, while the influence of the strong interaction encoded in T_{VN} is, within the QCD sum rule approach, of sub-leading order, for the given examples.

C Spectral functions

While the global mass shifts of the in-medium ρ and ω mesons are governed mainly by the strength of the 4-quark condensate density dependence, the details of the vector meson spectral functions depend also on the meson-nucleon scattering amplitude T_{VN}. In Fig. 5 we plot the ρ meson spectral density for $\kappa_N = 1 \cdots 3$ at normal nuclear density. (Note that the spectral functions determine the emission of di-electrons from the vector meson decays [9, 30].) The main trend of the down shift of the ρ meson spectral function peak position is in accordance with the dropping ρ meson mass obtained above by a stronger density dependence, parameterized by larger values of κ_N. When the peak of $S^{(\rho)}(E)$ is in the interval $E \simeq 0.4 \cdots 0.6$ GeV, i.e. for $\kappa_N \simeq 1 \cdots 3$, the width of the spectral function decreases as the peak moves to the smaller values of E. This is not a surprise if one takes into account the energy dependence of $\mathrm{Im}T_{\rho N}(E)$ in the same (subthreshold) energy interval (see Fig. 10), where $\mathrm{Im}T_{\rho N}(E)$ also drops with decreasing energy. From this one can also conclude that in a wide region of κ_N the ρ meson does not undergo drastic collision broadening at normal nuclear density, in contrast to earlier expectations but in line with [19].

In Fig. 6 we display the change of the ω meson spectral function in nuclear matter at normal nuclear density for the same parameters κ_N as for the ρ meson (see Fig. 5). The in-medium spectral change is still seen to be dominated by the density dependence of the 4-quark condensate. The dependence of the peak position on the parameter κ_N is similar to $m_\omega(n)$, namely, for a weak density dependence of the 4-quark condensate ($\kappa_N \lesssim 3$) the peak is up-shifted compared to vacuum, while for $\kappa_N \gtrsim 3$ the peak moves to a smaller value of the energy. For $S^{(\omega)}(E)$ with up-shifted peak positions the width remains almost constant. This is in agreement with the approximately constant value of $\mathrm{Im}T_{\omega N}(E)$ in the region $E \gtrsim 0.8$ GeV (see Fig. 11). When the peak of $S^{(\omega)}(E)$ moves to a smaller energy (for $\kappa_N \gtrsim 3$) the width of the ω meson increases moderately, which is caused by the increase of $\mathrm{Im}T_{\omega N}(E)$ (see Fig. 11) in the corresponding interval of energy.

The pure hadronic calculation in [19] predicts a slight up-shift of the original ω peak. This case is reproduced in our approach by $\kappa_N \approx 2.7$. However, such a value of κ_N delivers a strong down-shift of the original ρ peak (see Fig. 5), at variance to the results in [19]. Otherwise, in contrast to [16], but in agreement with [19], the ρ width is less affected by in-medium effects; rather for a strongly decreasing ρ mass the width may even become smaller, as discussed above.

IV. ϕ MESON

The treatment of the ϕ meson proceeds along the same strategy as presented above. The corresponding current operator in eq. (2.1) is $J_\mu = \bar{s}\gamma_\mu s$ which renders the coefficients $c_{1,2,3}$ to be used in eq. (2.14) into

$$c_1 = -\frac{3m_s^2}{4\pi^2} \, , \tag{4.1}$$

$$c_2 = m_s \langle \bar{s}s \rangle_0 + y \frac{m_s \sigma_N}{2m_q} \, n + \frac{1}{24} \left[\langle \frac{\alpha_s}{\pi} G^2 \rangle_0 - \frac{8}{9} M_N^0 \, n \right] + \frac{1}{4} A_2^s M_N \, n \, , \tag{4.2}$$

$$c_3 = -\frac{112}{81} \pi \, \alpha_s \, \kappa_0 \, \langle \bar{s}s \rangle_0^2 \left[1 + \frac{\kappa_N}{\kappa_0} \frac{\sigma_N}{m_q \langle \bar{s}s \rangle_0} \, n \right] - \frac{5}{12} A_4^s M_N^3 \, n \, , \tag{4.3}$$

where c_0 is not changed. At the scale $\mu^2 = 1$ GeV^2 the condensates are $A_2^s = 0.05$ and $A_4^s = 0.002$ [11]. $y = \langle N|\bar{s}s|N\rangle / \langle N|\bar{q}q|N\rangle$ is the poorly known strangeness content of the nucleon which may vary from 0 to 0.25 [31]. We utilize here $y = 0.22$, as in [11]. Further parameters are $\langle \bar{s}s \rangle_0 = \hat{y} \langle \bar{q}q \rangle_0$ with $\hat{y} = 0.8$ and $m_s = 130$ MeV. The subtraction constant is negligible, i.e. $\Pi^{(\phi)}(0, n) = 0$ [32]. $\mathrm{Re}\Sigma_\phi^{\mathrm{vac}} - n\mathrm{Re}T_{\phi N}$ is absorbed again in $\overset{\circ}{m}_\phi\ (n)$, while $\mathrm{Im}\Sigma_\phi^{\mathrm{vac}}(E) = -m_\phi \Gamma_\phi \Theta(E - 2m_K))$ with vacuum parameters m_K, m_ϕ, Γ_ϕ. $M^2_{\mathrm{max}} = 3$ GeV^2 is dictated by the "50% rule".

For $\mathrm{Im}T_{\phi N}$ we employ the previous estimates [16] (see solid curve in figure 8 in first reference of [16]). Since this $\mathrm{Im}T_{\phi N}$ is comparatively large we find some weak dependence of m_ϕ on κ_N, see Fig. 7. The pattern of the κ_N dependence resembles the one of the ρ meson but is much more moderate. (Note that the slope of the curves $m_\phi(n)$ scale with y [33].) Since the used amplitude $T_{\phi N}$ shows minor variations at $E \sim m_\phi$, the widths of the shifted spectral functions is quite independent of κ_N, see Fig. 8. (When using the amplitude of [34] the width would become larger with increasing values of κ_N.)

V. SUMMARY AND DISCUSSION

In summary we present a systematic evaluation of the Borel QCD sum rule for ρ and ω mesons. We go beyond the often employed zero-width approximation and use a realistic ansatz for the spectral function. A crucial element for our analysis is the use of the recent ρ, ω meson-nucleon scattering amplitudes adjusted to a large data basis. These differ noticeably from earlier employed amplitudes. Despite of such differences, the results of our analysis are robust: The ρ meson suffers a down shift by an amount determined by the yet poorly known density dependence of the 4-quark condensates. The latter ones determine also whether the ω meson suffers an up-shift or a down-shift. One consequence of the scattering amplitudes [19] is a moderate in-medium broadening of the ρ, ω spectral functions, in contrast to earlier predictions. We focus on the region in the vicinity of the ρ, ω peaks in vacuum. Therefore, we do not address such problems as the development of second, low-energy peak in the ω strength, as found in [19].

Besides the exploration of the importance of the density dependence of the 4-quark condensates, the determination of the in-medium modification of ρ and ω on a common footing is the main objective of the present paper. This is highlighted in Fig. 9, which points to drastic shifts of either the ω meson or the ρ meson, or to still noticeable shifts of both. Fairly independent of κ_N is the $\rho - \omega$ mass splitting of about 200 MeV at normal nuclear matter density. (Using ImT_V from [16] results in a much smaller $\rho - \omega$ mass splitting which even disappears for $\kappa_N < 1$.) It should be stressed, however, that the use of a common parameter κ_N for the light vector mesons is an approximation, since actually ρ, ω and ϕ mesons have their own κ_N's. The detailed analysis deserves a separate investigation.

It turns out that the cross properties of the ρ and ω mesons are determined, to a large extent, by the condensates, while the meson-nucleon scattering amplitudes are still important for the quantitative behavior. Basing on this observation we consider also the ϕ meson using estimates of the ϕ meson-nucleon scattering amplitude. In contrast to the ρ, ω mesons, the in-medium modification of the ϕ meson is determined by the strangeness chiral condensate and depends essentially on the strangeness content of the nucleon.

In our approach we rely on the linear density approximation. There are examples in the literature (e.g. [35]) which show that, e.g., the chiral condensate begins to deviate from the linear density behavior at normal nuclear matter density. Resting on this argument one can expect the quantitative validity of our results up to n_0.

We have truncated, according to the common praxis, the OPE at order 3. Higher-order terms are not yet calculated in a systematic way. This issue needs further consideration, as also the case of a finite spatial momentum of the vector mesons [36].

Concerning an experimental opportunity to observe both ρ and ω mesons in-medium mass shifts simultaneously in heavy-ion collisions, our analysis still shows the crucial importance of the in-medium density dependence of the 4-quark condensate. In particular, if the 4-quark condensate density dependence is not too strong (i.e. for $\kappa_n \stackrel{\sim}{<} 2$) there is a chance to observe the up-shifted peak of the ω resonance, while the ρ meson is down-shifted. The measurements with HADES, once the ρ and ω peaks are identified, will constrain the mentioned important density dependence of the 4-quark condensates and, consequently, the strength of approaching chiral symmetry restoration.

Acknowledgments: We thank E.G. Drukarev, R. Hofmann, S. Leupold, V.I. Zakharov, and G.M. Zinovjev for useful discussions. We are especially grateful to M.F.M. Lutz and Gy. Wolf for discussions on the results of [19] and for supplying the information of T_{VN}. O.P.P. acknowledges the warm hospitality of the nuclear theory group in the Research Center Rossendorf. This work is supported by BMBF 06DR121, STCU 15a, CERN-INTAS 2000-349, NATO-2000-PST CLG 977 482.

APPENDIX A: SELF-ENERGY OF ρ MESON IN VACUUM

The self-energy of ρ meson in vacuum is $\Sigma_\rho^{\rm vac}(q) = \frac{1}{3}\, g_{\mu\nu}\, \Sigma^{\mu\nu}(q)$ where the self-energy tensor $\Sigma^{\mu\nu}(q)$ within an effective Lagrangian for the $\rho\pi\pi$ interaction is given by [30]

$$i\, \Sigma^{\mu\nu}(q) = g_{\rho\pi\pi}^2 \int \frac{d^4p}{(2\pi)^4} \, \frac{1}{[p^2 - m_\pi^2 + i\epsilon]} \, \left(\frac{(2p-q)^\mu \, (2p-q)^\nu}{[(p-q)^2 - m_\pi^2 + i\epsilon]} - \, 2g^{\mu\nu} \right) \quad \text{(A.1)}$$

with the coupling constant $g_{\rho\pi\pi} = 5.79$ and $m_\pi = 0.138$ GeV. Using the renormalization scheme of [19, 37] we get for the meson at rest, i.e. $q = (E, \mathbf{0})$,

$$\begin{aligned} \Sigma_\rho^{\rm vac}(E) = \frac{g_{\rho\pi\pi}^2}{48\pi^2}\, (4m_\pi^2 - E^2) \Bigg\{ & \sqrt{1 - \frac{4m_\pi^2}{E^2}} \, \ln \left(\frac{\sqrt{1 - \frac{4m_\pi^2}{E^2}} - 1}{\sqrt{1 - \frac{4m_\pi^2}{E^2}} + 1} \right) \\ & - \sqrt{1 - \frac{4m_\pi^2}{m_\rho^2(0)}} \, \ln \left(\frac{1 - \sqrt{1 - \frac{4m_\pi^2}{m_\rho^2(0)}}}{1 + \sqrt{1 - \frac{4m_\pi^2}{m_\rho^2(0)}}} \right) \Bigg\} \, , \end{aligned} \quad \text{(A.2)}$$

where $m_\rho(0) = 0.769$ GeV is the vacuum mass of ρ meson. In this scheme, $m_\rho(0) = \stackrel{\circ}{m}_\rho(0)$ follows from eq. (2.12).

APPENDIX B: ρ, ω - NUCLEON SCATTERING AMPLITUDES

For definiteness we plot in Figs. 10 and 11 the spin and isospin averaged amplitudes for ρ and ω mesons, respectively, which are employed in our QSR evaluations and not explicitly given in [19].

APPENDIX C: TECHNICAL DETAILS

Here we would like to report a few technical details of our sum rule evaluation. Let us first consider the density dependence of the continuum threshold, see Figs. 12 and 13. When changing the density, but keeping the rules for the Borel window as described above, the continuum thresholds s_V change. The overall pattern resembles the behavior of $\overset{\circ}{m}_V$: a decreasing (increasing) $\overset{\circ}{m}_V$ implies a decreasing (increasing) s_V.

If one would freeze the continuum thresholds to the vacuum values, i.e., $s_V(n) = s_V(0)$, the $\rho - \omega$ mass splitting at normal nuclear matter density is reduced to about 100 MeV and the dependence on κ_N becomes much weaker.

Next we consider the stability of our results with respect of the choice of the Borel window at normal nuclear matter density. Figs. 14 and 15 exhibit the change of the parameter $\overset{\circ}{m}_V$ when changing $M^2_{\rm min}$. As expected, $\overset{\circ}{m}_V$ slightly increases with decreasing $M^2_{\rm min}$ (compare also with Figs. 1 and 2). The change is fairly moderate but points to some dependence of the absolute values of $\overset{\circ}{m}_V$ and m_V on the Borel window. This, however, is not important since our focus here is the pattern of the in-medium modification and not absolute predictions, which are hampered anyhow by the uncertainty related with the 4-quark condensate. A similar statement holds for changes of $M^2_{\rm max}$, see Figs. 16 and 17. With virtue to Figs. 1 and 2 the decrease of $\overset{\circ}{m}_V$ with increasing $M^2_{\rm max}$ is counter-intuitive. The explanation of this behavior comes from the change of s_V when changing $M^2_{\rm max}$. When directly determining $M^2_{\rm max}$ by the "50 % rule" [22, 29] we arrive at a sliding Borel window.

REFERENCES

[1] J. Friese (for the HADES collaboration), Prog. Part. Nucl. Phys. **42** (1999) 235; http://www-hades.gsi.de.

[2] S. Weinberg, Phys. Rev. Lett. **18** (1967) 507;
J. Kapusta, E. V. Shuryak, Phys. Rev. **D 49** (1994) 4696.

[3] M. Dey, V. L. Eletsky, B. L. Ioffe, Phys. Lett. **252** (1990) 620.

[4] F. Karsch, Nucl. Phys. **B 83** (Proc. Suppl.) (2000) 14.

[5] T. Hatsuda, T. Kunihiro, M. Shimizu, Phys. Rev. Lett. **82** (1999) 2840;
T. Hatsuda, Nucl. Phys. **A 698** (2002) 243c.

[6] G. E. Brown, M. Rho, Phys. Rep. **363** (2002) 82.

[7] M. Harada, C. Sasaki, Phys. Lett. **B 537** (2002) 280.

[8] G. E. Brown, M. Rho, nucl-th/0206021.

[9] R. Rapp, J. Wambach, Adv. Nucl. Phys. **25** (2000) 1.

[10] P. Finelli, N. Kaiser, D. Vretenar, W. Weise, nucl-th/0205016.

[11] T. Hatsuda, S. H. Lee, Phys. Rev. **C 46** (1992) R 34;
T. Hatsuda, S. H. Lee, H. Shiomi, Phys. Rev. **C 52** (1995) 3364.

[12] M. A. Shifman, A. I. Vainshtein, V. I. Zakharov, Nucl. Phys. **B 147** (1979) 385.

[13] S. Leupold, W. Peters, U. Mosel, Nucl. Phys. **A 628** (1998) 311.

[14] S. Zschocke, O. P. Pavlenko, B. Kämpfer, Eur. Phys. J. **A 15** (2002) 529.

[15] S. Zschocke, O. P. Pavlenko, B. Kämpfer, Phys. Lett. **B 562** (2003) 57.

[16] F. Klingl, N. Kaiser, W. Weise, Nucl. Phys. **A 624** (1997) 527;
F. Klingl, T. Waas, W. Weise, Nucl. Phys. **A 650** (1999) 299.

[17] W. Cassing. E. L. Bratkovskaya, Phys. Rep. **308** (1999) 65;
Gy. Wolf, O. P. Pavlenko, B. Kämpfer, nucl-th/0306029.

[18] B. Kämpfer, O. P. Pavlenko, Eur. Phys. J. **A 10** (2001) 101.

[19] M. F. M. Lutz, Gy. Wolf, B. Friman, Nucl. Phys. **A 706** (2002) 431.

[20] A. K. Dutt-Mazumder, R. Hofmann, M. Pospelov, Phys. Rev. **C 63** (2000)

015204.

[21] T. Hatsuda, Y. Koike, S. H. Lee, Nucl. Phys. **B 394** (1993) 221.

[22] S. Leupold, U. Mosel, Phys. Rev. **C 58** (1998) 2939;
S. Leupold, Phys. Rev. **C 64** (2001) 015202.

[23] E. G. Drukarev, M. G. Ryskin, V. A. Sadovnikova, V. E. Lyubovitskij, T. Gutsche, A. Faessler, hep-ph/0306132.

[24] M. A. Shifman, A. I. Vainshtein, V. I. Zakharov, Nucl. Phys. **B 147** (1979) 448.

[25] T. D. Cohen, R. J. Furnstahl, D. K. Griegel, X. Jin, Prog. Part. Nucl. Phys. **35** (1995) 221.

[26] M. Asakawa, C. M. Ko, Phys. Rev. **C 48** (1993) R 526, Nucl. Phys. **A 560** (1993) 399.

[27] F. Klingl, N. Kaiser, W. Weise, Z. Phys. **A 356** (1996) 193.

[28] W. Florkowski, W. Broniowski, Nucl. Phys. **A 651** (1999) 397.

[29] X. Jin, D. B. Leinweber, Phys. Rev. **C 52** (1995) 3344;
D. B. Leinweber, Ann. Phys. **254** (1997) 328.

[30] C. Gale, J. Kapusta, Nucl. Phys. **B 357** (1991) 65.

[31] K. F. Liu, S. J. Dong, T. Draper, D. Leinweber, J. Sloan, W. Wilcox, R. M. Woloshyn, Phys. Rev. **D 59** (2001) 11;
C. Michael, C. McNeile, D. Hepburn, Nucl. Phys. Proc. Suppl. **106** (2002) 293;
W. M. Alberico, S. M. Bilenky, C. Maieron, Phys. Rep. **358** (2002) 227.

[32] M. Askawa, C.M. Ko, Nucl. Phys. **A 572** (1994) 732.

[33] B. Kämpfer, O.P. Pavlenko, S. Zschocke, Eur. Phys. J. **A 17** (2003) 83.

[34] F. Klingl, T. Waas, W. Weise, Phys. Lett. **B 431** (1998) 254.

[35] M. Lutz, B. Friman, C. Appel, Phys. Lett. **474** (2000) 7.

[36] M. Post, S. Leupold, U. Mosel, Nucl. Phys. **A 689** (2001) 753;
H. S. Lee, H. C. Kim, Nucl. Phys. **A 642** (1998) 165.

[37] T. Fuchs, J. Gegelia, G. Japaridze, S. Scherer, hep-ph/0302117.

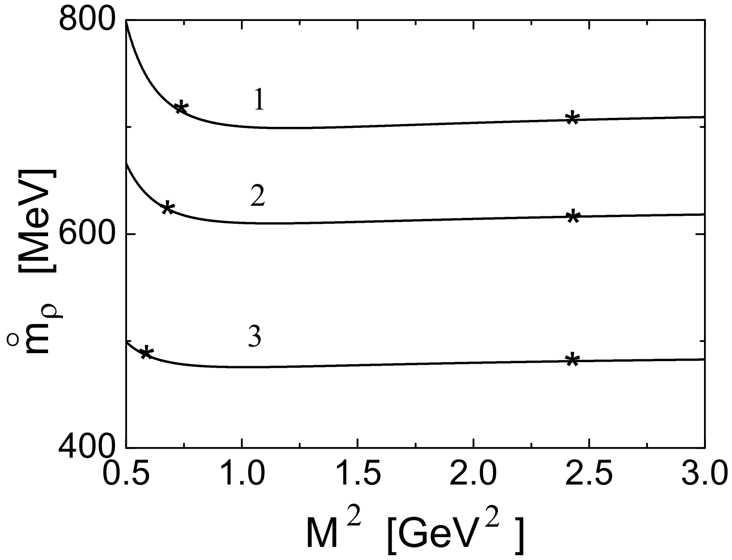

FIG. 1: The ρ meson mass parameter $\overset{\circ}{m}_\rho$ as a function of the Borel parameter M^2. The respective continuum thresholds $s_\rho = 1.13, 0.92$, and 0.65 GeV^2 for $\kappa_N = 1, 2$ and 3 follow from the maximum flatness requirement within the Borel window (marked by stars) defined here by $M^2_{\rm min}(10\%)$ and $M^2_{\rm max} = 2.4$ GeV^2. $n = n_0$.

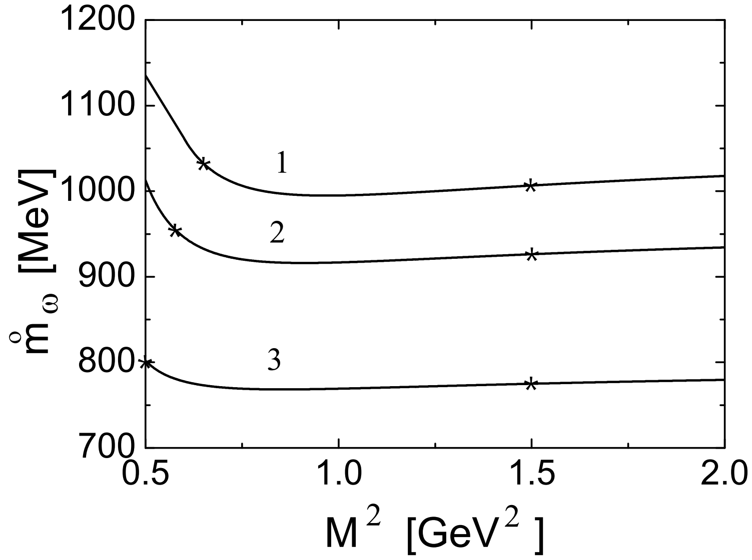

FIG. 2: As in Fig. 1, but for ω meson. $M^2_{\rm max} = 1.5$ GeV^2.

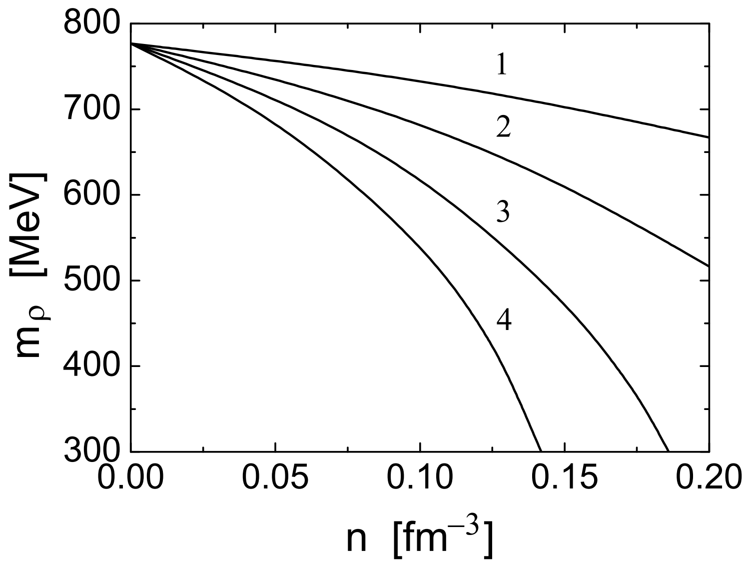

FIG. 3: Density dependence of the ρ meson mass for various values of the parameter κ_N.

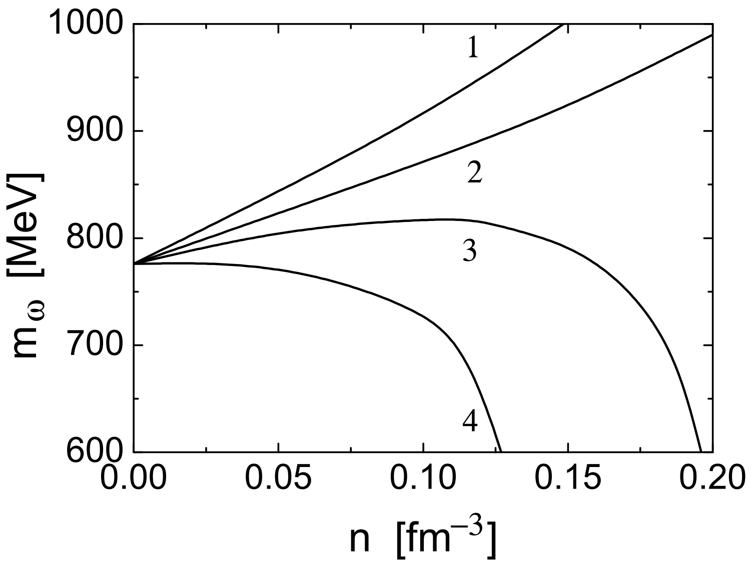

FIG. 4: As in Fig. 3, but for ω meson.

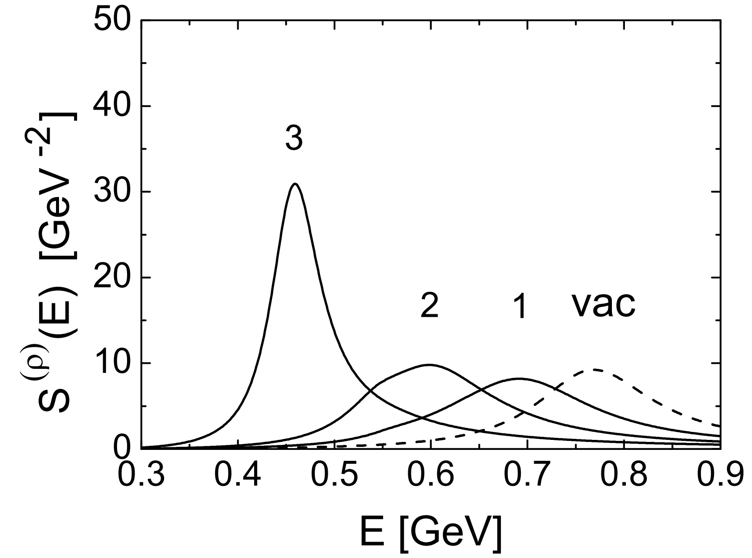

FIG. 5: ρ meson spectral density for $\kappa_N = 1...3$. Solid curves correspond to normal nuclear density, while the dashed curve is for vacuum.

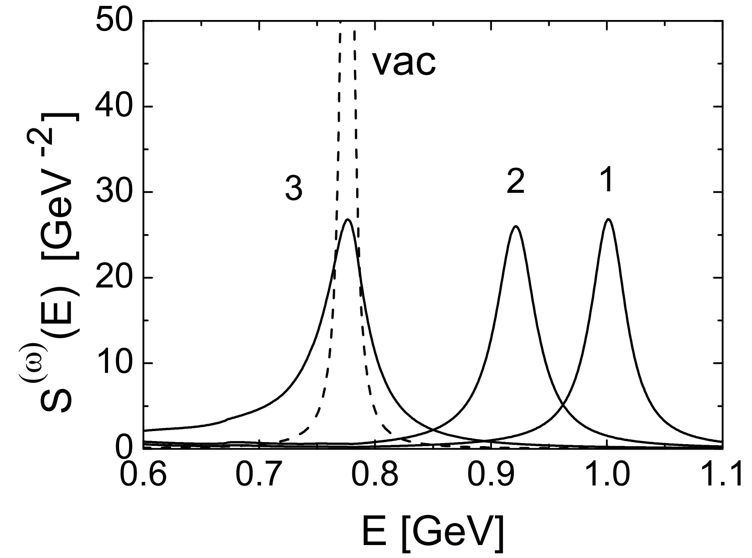

FIG. 6: As in Fig. 5, but for ω meson.

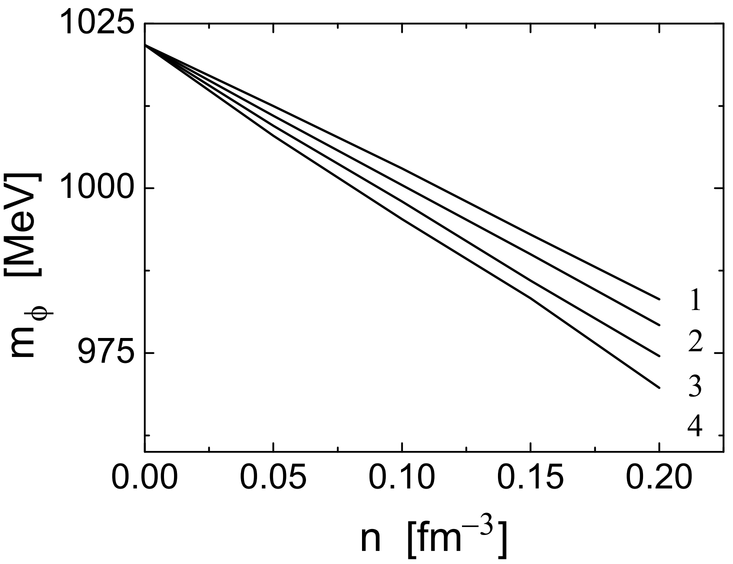

FIG. 7: As in Fig. 3, but for ϕ meson.

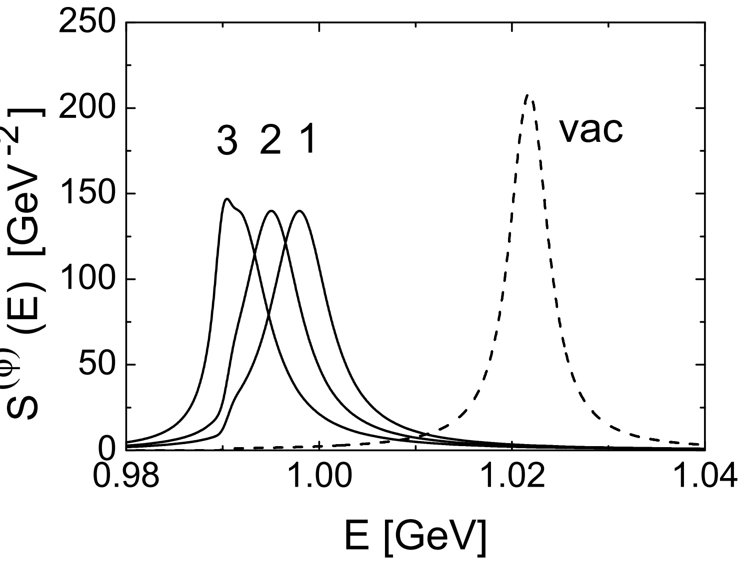

FIG. 8: As in Fig. 5, but for ϕ meson.

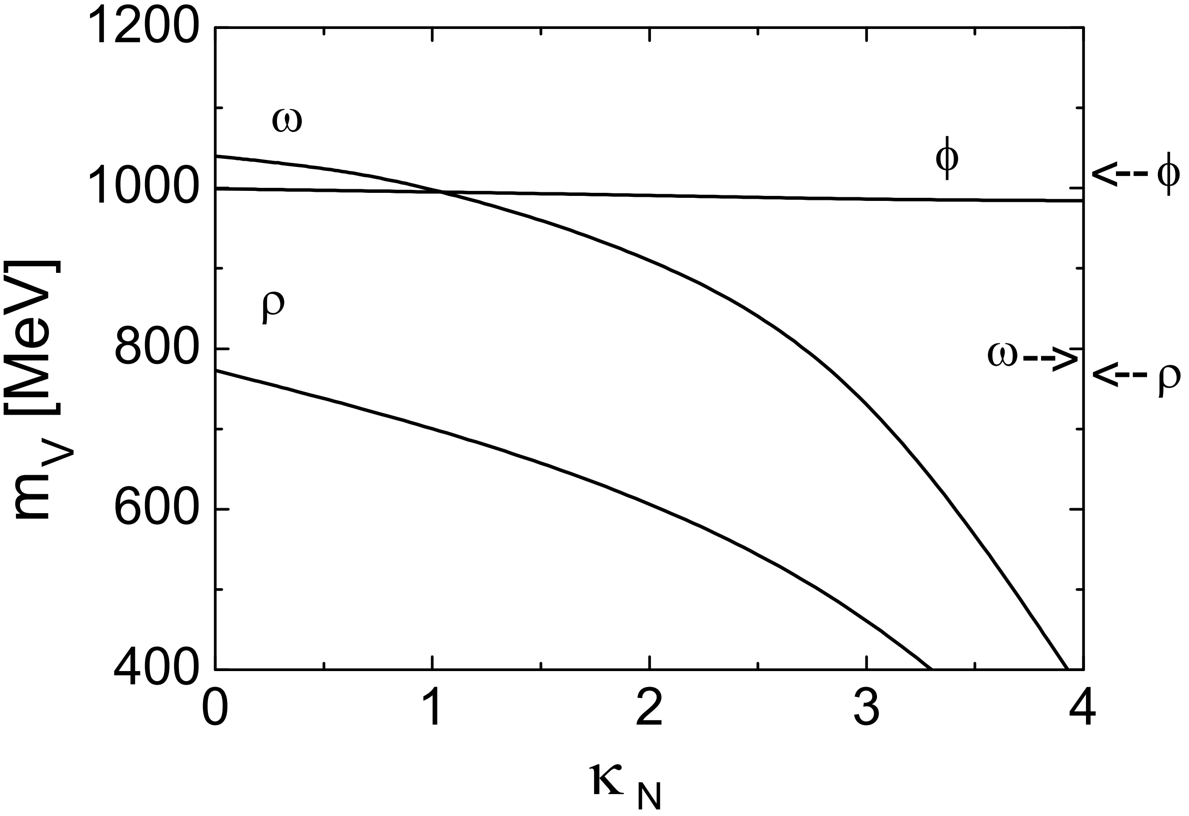

FIG. 9: Dependence of the vector meson masses on the parameter κ_N at normal nuclear matter density. The arrows depict the vacuum masses.

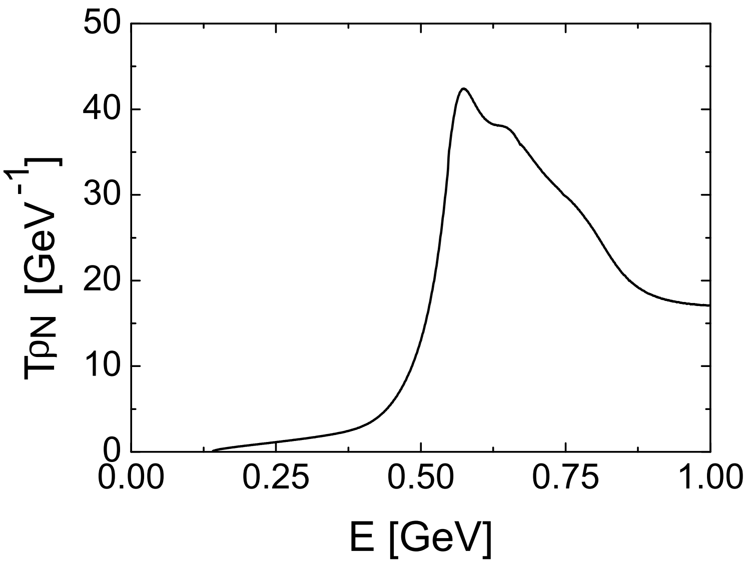

FIG. 10: Imaginary part of the spin and isospin averaged ρ meson-nucleon scattering amplitude for the approach of [19].

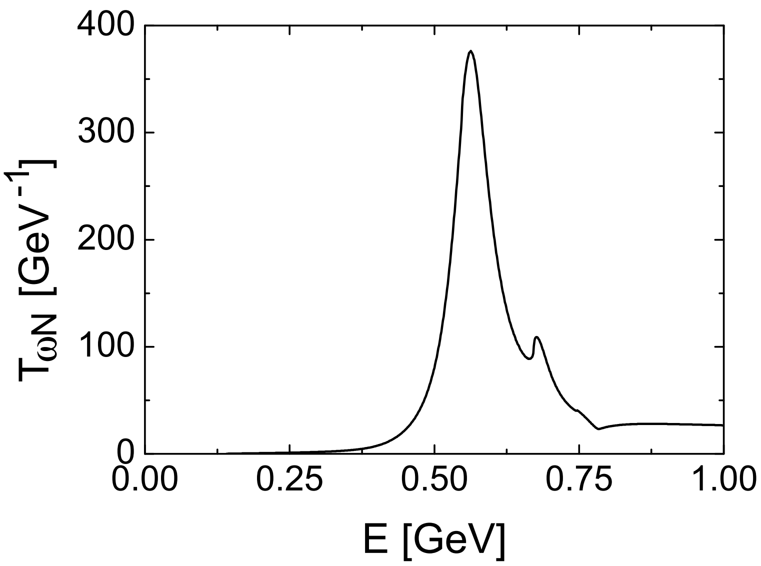

FIG. 11: As in Fig. 10, but for ω meson.

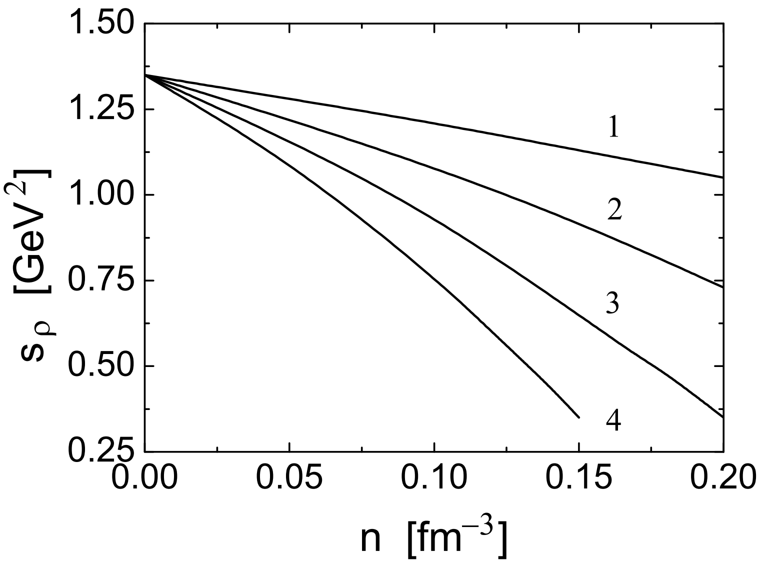

FIG. 12: Density dependence of the continuum threshold s_ρ for various values of the parameter κ_N.

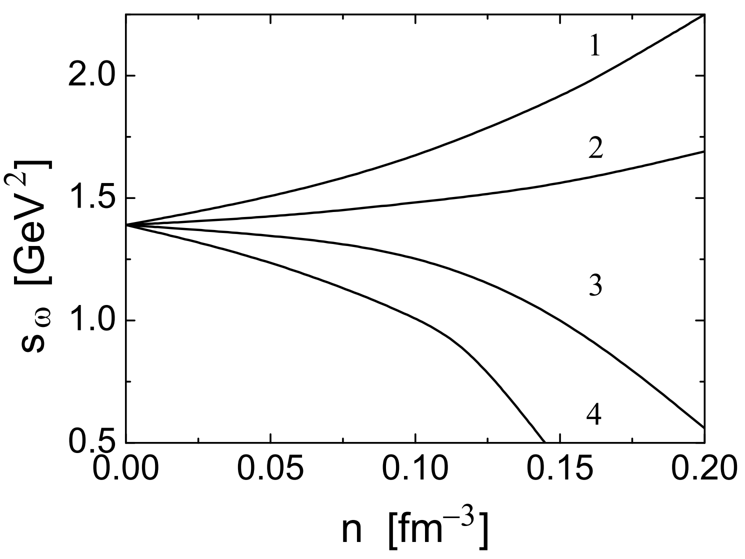

FIG. 13: As in Fig. 12, but for ω meson.

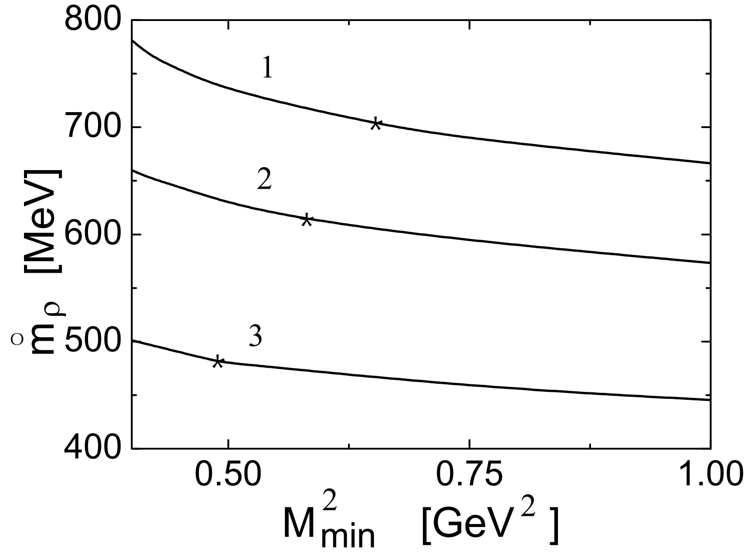

FIG. 14: The parameter $\overset{o}{m}_\rho$ as a function of the minimum Borel parameter $M_{\rm min}$. $M^2_{\rm max} = 2.4$ GeV^2. The stars mark $M^2_{\rm min}(10\%)$. $n = n_0$.

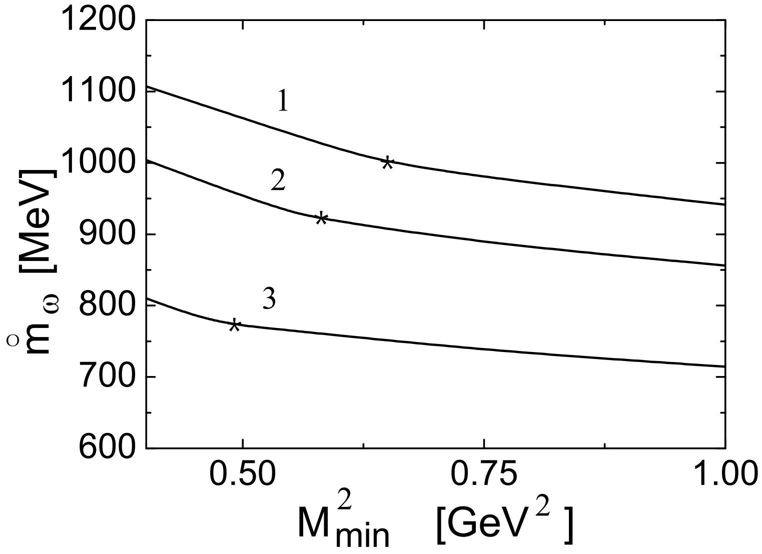

FIG. 15: As in Fig. 14, but for ω meson. $M^2_{\rm max} = 1.5$ GeV^2.

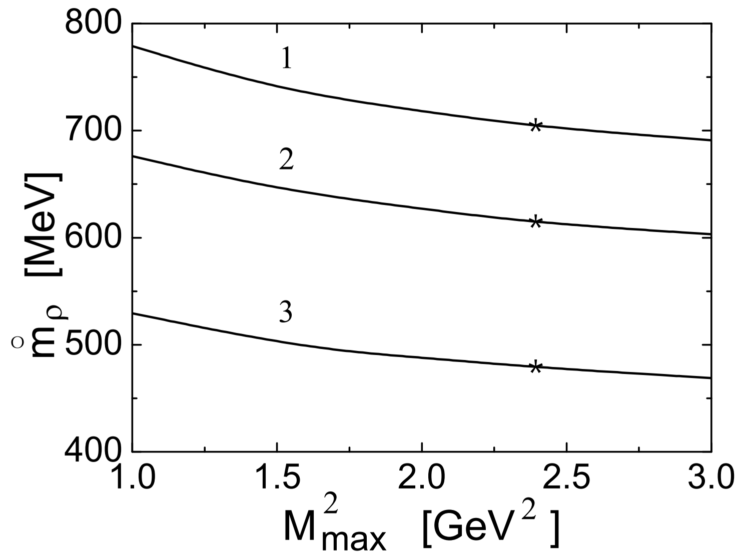

FIG. 16: The parameter $\overset{\circ}{m}_\rho$ as a function of the maximum Borel parameter $M^2_{\rm max}$. The minimum Borel parameter is $M^2_{\rm min}(10\%)$. The stars mark $M^2_{\rm max} = 2.4$ GeV^2. $n = n_0$.

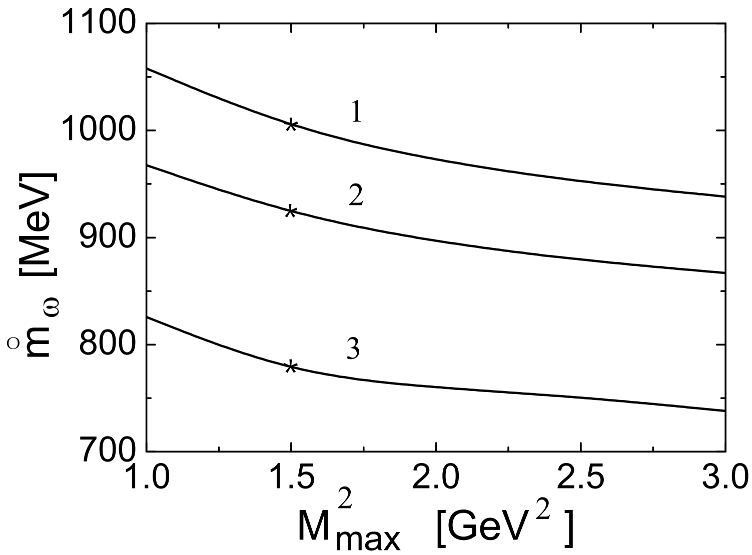

FIG. 17: As in Fig. 16, but for ω meson. The stars mark $M^2_{\rm max} = 1.5$ GeV^2.